Tidal decay and orbital circularization in close-in two-planet systems

A. Rodríguez,[1]⋆ S. Ferraz-Mello,[1] T. A. Michtchenko,[1] C. Beaugé[2] and O. Miloni[3]

[1]*Insituto de Astronomia, Geofísica e Ciências Atmosféricas, IAG-USP, Rua do Matão 1226, 05508-900 São Paulo, Brazil*
[2]*Observatório Astronómico, Universidad Nacional de Córdoba, Laprida 854, (X5000BGR) Córdoba, Argentina*
[3]*Facultad de Ciencias Astronómicas y Geofísicas, Universidad Nacional de La Plata, Paseo del Bosque S/N B1900 FWA, La Plata, Argentina*

ABSTRACT

The motion of two planets around a Sun-like star under the combined effects of mutual interaction and tidal dissipation is investigated. The secular behaviour of the system is analysed using two different approaches. First, we solve the exact equations of motion through the numerical simulation of the system evolution. In addition to the orbital decay and circularization, we show that the final configuration of the system is affected by the shrinking of the inner orbit. Our second approach consists of the analysis of the stationary solutions of mean equations of motion based on a Hamiltonian formalism.

We consider the case of a hot super-Earth planet with a more massive outer companion. As a real example, the CoRoT-7 system is analysed, solving the exact and mean equations of motion. The star–planet tidal interaction produces orbital decay and circularization of the orbit of CoRoT-7b. In addition, the long-term tidal evolution is such that the eccentricity of CoRoT-7c is also circularized and a pair of final circular orbits is obtained. A curve in the space of eccentricities can be constructed through the computation of stationary solutions of mean equations including dissipation. The application to the CoRoT-7 system shows that the stationary curve agrees with the result of numerical simulations of exact equations.

A similar investigation performed in a super-Earth–Jupiter two-planet system shows that the doubly circular state is accelerated when there is a significant orbital migration of the inner planet, in comparison with previous results where migration is neglected.

Key words: celestial mechanics – planetary systems.

1 INTRODUCTION

It is well known that close-in planets undergo tidal interactions with their host stars. The tidal effect produces orbital decay, circularization and spin–orbit synchronization of a planet orbiting a slow-rotating star (Dobbs-Dixon, Lin & Mardling 2004; Ferraz-Mello, Rodríguez & Hussmann 2008; Jackson, Greenberg & Barnes 2008). When the tidally affected planet has an eccentric companion, its evolution is more complicated. As we shall show in this paper for two different systems, new features appear due to the interplay of tidal effects and mutual interactions between planets.

Several works have already investigated the evolution of two-planet systems accounting for the tidal dissipation (Wu & Goldreich 2002; Mardling & Lin 2004; Mardling 2007; Zhou & Lin 2008; Mardling 2010; Greenberg & Van Laerhoven 2011). Particularly in Mardling (2007), a secular model based on the Legendre expansion of the disturbing forces up to the fourth order in semimajor axis ratio, a_1/a_2, was introduced. She has shown that the outer companion excites the eccentricity of the inner planet, accelerating its

migration towards the star due to the tidal dissipation. Moreover, the evolution of the system under the tidal effect follows several stages, depending on the circulation or oscillation of the angle between the lines of apses. The excitation of the inner planet eccentricity reaches a quasi-equilibrium value and, on a long time-scale (which depends on physical parameters and initial orbital configuration), both eccentricities are damped to zero. If the companion planet can sustain a non-zero eccentricity of the inner planet for times of the order of the age of the system, the mechanism could explain some observed oversized planets, since the body can inflate in response to tidal heat. The companion planet hypothesis would thus explain the large size of some planets, e.g. HD 209458b, HAT-P1b and WASP-1b (see Mardling 2007 for details).

Although Mardling's model has no restrictions on the values of the planetary mass ratio, its applications have given priority to systems with more massive inner planets.[1] In this case, in a first approximation, we may assume that the planetary semimajor axes do not vary during the tidal evolution. This approximation

---

⋆ E-mail: adrian@astro.iag.usp.br

---

[1] Except in the case of the HAT-P-13 non-coplanar system (see Mardling 2010).

may be sufficient for systems with a less massive outer planet, in which case the excitation of the inner planet eccentricity is not strong enough to induce its rapid orbital decay due to tidal friction. As a consequence, the orbital decay of the inner planet occurs on time-scales much longer than the ages of the systems analysed in Mardling (2007). In this scenario, analytical results have shown a good agreement with results of numerical simulations, performed through numerical integrations of Lagrange's planetary equations.

In the present work, we use a different approach, with no restrictions on the semimajor axis variation, which allows us to investigate the tidal evolution of two-planet systems with an arbitrary mass ratio. We perform numerical simulations using Newton's equations of the coplanar motion of two planets and including the forces due to tidal friction according to Mignard (1979). We show that the angular momentum conservation constrains the variation of the planetary orbital elements, even in the case of a rapid orbital decay.

We perform an adaptation of the conservative analytical model of secular motion to the systems with slow loss of energy, such as a tidally affected pair of planets. Assuming that the planets are far enough from any mean-motion resonances, only secular terms are maintained in the disturbing function. Previous works have shown that for a given value of the total angular momentum, all possible motions of the secular system are constant-amplitude oscillations around one of the two equilibria of the secular Hamiltonian, known as Mode I and Mode II (Michtchenko & Ferraz-Mello 2001; Michtchenko & Malhotra 2004). We also know that the location of the stationary solutions in the phase space is uniquely defined by two parameters: the ratios of planet masses and semimajor axes.

When we consider the non-conservative secular system, in which the rate of dissipation is sufficiently slow (more precisely, it is slower than the proper frequency of the system), the parameter a_1/a_2 varies slightly due to the slow orbital decay of the inner planet. For all possible values of a_1/a_2 and the total angular momentum, we may calculate the locations of the equilibria in the phase space. A curve of stationary solutions can be constructed and then compared with the result of numerical simulation of the system (see Michtchenko & Rodríguez 2011 for a detailed discussion).

In this paper, we restrict our investigations to systems with a hot super-Earth and a more massive outer companion. By super-Earth, we mean planets with an upper limit of $10 \, m_\oplus$, where $m_\oplus$ is the mass of the Earth (Fortney, Marley & Barnes 2007; Valencia, Sasselov & O'Connell 2007). To date, 24 known super-Earths have been discovered with masses ranging from 1.94 to $9.22 \, m_\oplus$ and the majority of these planets evolve in multi-planet systems.[2] Almost half of the known super-Earths have orbital periods smaller than 5 d; so small periods indicate that the planets have experienced an orbital decay due to tidal interaction with the star.

We apply our approach to the CoRoT-7 extrasolar system, which is composed of one super-Earth and a more massive outer companion (Queloz et al. 2009; Léger at al. 2009; Ferraz-Mello et al. 2011). Previous investigations involving the tidal evolution of CoRoT-7 planets include the analysis of the tidal heating of CoRoT-7b and the consequences for its orbital migration. It was shown that the past history of the planet may have included a tidal heating large enough to be compared with the corresponding tidal heating of the Jovian satellite Io (Barnes et al. 2010). The coupled interaction between tides and the secular evolution in the CoRoT-7 system is investigated in this paper, showing that a final orbital configuration with

two circular orbits is obtained in a few Myr. This is one of the main aims of this paper.

This paper is organized as follows. In Section 2, we briefly describe the tidal evolution for a single-planet system. In Section 3 we analyse the two-planet secular behaviour through numerical integrations of the exact equations of motion including the tidal force (in the coplanar case). We consider two applications: the real system CoRoT-7 and a hypothetical system containing a hot super-Earth with a Jupiter companion. The angular momentum conservation of the system is discussed in Section 4, providing a simple explanation for the damping of the outer planet eccentricity and the orbital decay of the inner planet. In Section 5, we investigate the secular dynamics of CoRoT-7 planets through the study of stationary solutions of the mean equations using the Hamiltonian formalism. The role of stellar tides is analysed in Section 6. Finally, Section 7 is devoted a general discussion and conclusions.

2 TIDAL EVOLUTION OF SINGLE PLANET

We first consider the tidal interaction between one planet and its host star. We call m_0 and R_0 the mass and stellar radius, whereas m_1 and R_1 are the corresponding planetary values. In the case of zero orbital inclination, the mean variations of orbital elements produced by the joint effect of both planetary and stellar tides are given by

$$\langle \dot{a} \rangle = -\frac{4}{3} n a^{-4} \hat{s} [(1 + 23e^2) + 7e^2 D] \qquad (1)$$

and

$$\langle \dot{e} \rangle = -\frac{2}{3} n e a^{-5} \hat{s} [9 + 7D], \qquad (2)$$

where $D \equiv \hat{p}/2\hat{s}$ and

$$\hat{s} \equiv \frac{9}{4} \frac{k_0}{Q_0} \frac{m_1}{m_0} R_0^5, \quad \hat{p} \equiv \frac{9}{2} \frac{k_1}{Q_1} \frac{m_0}{m_1} R_1^5 \qquad (3)$$

are the strengths of the stellar and planetary tides, respectively (Dobbs-Dixon et al. 2004; Ferraz-Mello et al. 2008). In the above equations, a, e and n are semimajor axis, eccentricity and mean orbital motion, respectively. k_i and Q_i are the Love number and dissipation function of the deformed body, for $i = 0, 1$. The dissipation function is associated with the efficiency for which the energy is dissipated in the interior of the tidally deformed body. The results are valid up to second order in eccentricity, assuming a quasi-synchronous planetary rotation and a slow-rotating star (see Section 3.2.3). To obtain the variations produced by stellar tide, a linear model with constant time lag was assumed to relate phase lags and tidal frequencies (see Section 3.1).

From equations (1) and (2) we obtain $da/a = F(e, D)de/e$, where

$$F(e, D) \equiv \frac{2[1 + (7D + 23)e^2]}{7D + 9}. \qquad (4)$$

After integration, we obtain

$$a = a_{\mathrm{ini}} \exp \left[\frac{(7D + 23) \left(e^2 - e_{\mathrm{ini}}^2 \right) + 2 \log \left(e/e_{\mathrm{ini}} \right)}{7D + 9} \right], \qquad (5)$$

where the subscript 'ini' indicates initial values. It should be emphasized that, when stellar tide is neglected ($D \to \infty$), we have

$$a = a_{\mathrm{ini}} \exp \left(e^2 - e_{\mathrm{ini}}^2 \right), \qquad (6)$$

indicating that the final position of the planet is completely determined by initial values of the elements.

It is important to note from equations (1) and (2) that the cumulative effect of tides produces orbital decay and circularization

---

[2] http://exoplanet.eu/

on time-scales which depend on the values of k_i/Q_i (see Jackson et al. 2008; Rodríguez & Ferraz-Mello 2010). Moreover, the stellar tide is the only source of orbital decay after total circularization is achieved. However, we see from equation (3) that the strength of the stellar tide is proportional to the planetary mass m_1. Hence, tides on the star due to large planets are more efficient than tides produced by small planets, in order to induce a planetary migration on time-scales comparable to the age of the system.

3 NUMERICAL SIMULATIONS OF THE TIDAL EVOLUTION OF TWO-PLANET SYSTEMS

In this section, we study the dynamical evolution of a system composed of two planets orbiting a central star. The purpose is to investigate how the presence of an outer companion affects the tidal evolution of the inner planet.

3.1 Numerical model

We will consider systems in which the inner planet is a super-Earth. As discussed in the previous section, in this case, the contribution due to stellar tides is negligible due to the small planet mass. We assume that both planets are deformed under the tides raised by the central star. In addition to the tidal force, we consider that the inner planet is also affected by the correction of the Newtonian potential of the star due to general relativity. The reference frame chosen is centred in the star (see Fig. 1) and the motion of the planets occurs in the reference plane (i.e. coplanar motion).

According to our assumptions, the orbits evolve under the combined effects of mutual interaction and tides raised by the star. The equations of motion of the planets are written as

$$\ddot{\boldsymbol{r}}_1 = -\frac{G(m_0 + m_1)}{r_1^3}\boldsymbol{r}_1 + Gm_2\left(\frac{\boldsymbol{r}_2 - \boldsymbol{r}_1}{|\boldsymbol{r}_2 - \boldsymbol{r}_1|^3} - \frac{\boldsymbol{r}_2}{r_2^3}\right)$$
$$+ \frac{(m_0 + m_1)}{m_0 m_1}(\boldsymbol{f} + \boldsymbol{f}_{\text{rel}}) + \frac{\boldsymbol{g}}{m_0}, \quad (7)$$

$$\ddot{\boldsymbol{r}}_2 = -\frac{G(m_0 + m_2)}{r_2^3}\boldsymbol{r}_2 + Gm_1\left(\frac{\boldsymbol{r}_1 - \boldsymbol{r}_2}{|\boldsymbol{r}_1 - \boldsymbol{r}_2|^3} - \frac{\boldsymbol{r}_1}{r_1^3}\right)$$
$$+ \frac{(m_0 + m_2)}{m_0 m_2}\boldsymbol{g} + \frac{(\boldsymbol{f} + \boldsymbol{f}_{\text{rel}})}{m_0}, \quad (8)$$

where $\boldsymbol{f}_{\text{rel}}$ is the general relativity contribution acting on the inner planet, which is approximately given by

$$\boldsymbol{f}_{\text{rel}} = \frac{Gm_1m_0}{c^2 r_1^3}\left[\left(4\frac{Gm_0}{r_1} - v_1^2\right)\boldsymbol{r}_1 + 4(\boldsymbol{r}_1 \cdot \boldsymbol{v}_1)\boldsymbol{v}_1\right] \quad (9)$$

where $\boldsymbol{v}_1 = \dot{\boldsymbol{r}}_1$ and c is the speed of light (see Beutler 2005). $\boldsymbol{f}$ and $\boldsymbol{g}$ are the tidal forces acting on the masses m_1 and m_2, respectively. We use the expression for tidal forces given by Mignard (1979):

$$\boldsymbol{f} = -3k_1\Delta t_1 \frac{Gm_0^2 R_1^5}{r_1^{10}}\left[2\boldsymbol{r}_1(\boldsymbol{r}_1 \cdot \boldsymbol{v}_1) + r_1^2(\boldsymbol{r}_1 \times \boldsymbol{\Omega}_1 + \boldsymbol{v}_1)\right], \quad (10)$$
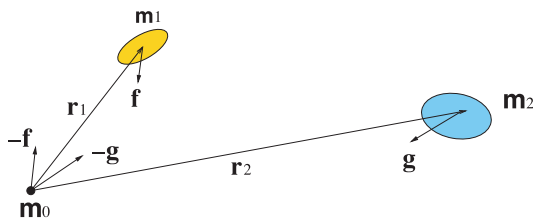

Figure 1. Schematic illustration of the tidal interaction in the system.

Table 1. The adopted orbital elements and physical data of the CoRoT-7 system (Léger et al. 2009; Queloz et al. 2009, Ferraz-Mello et al. 2011). The value of R_2 was computed assuming an Earth mean density for CoRoT-7c.

Body	m_i	R_i	$a_{i\,\text{current}}$ (au)	$e_{i\,\text{current}}$	Q'_i
0	$0.93\,\text{m}_\odot$	$0.87\,\text{R}_\odot$	–	–	–
1	$8.0\,m_\oplus$	$1.58\,R_\oplus$	0.017	0	100
2	$13.6\,m_\oplus$	$2.39\,R_\oplus$	0.046	0	100

$$\boldsymbol{g} = -3k_2\Delta t_2 \frac{Gm_0^2 R_2^5}{r_2^{10}}\left[2\boldsymbol{r}_2(\boldsymbol{r}_2 \cdot \boldsymbol{v}_2) + r_2^2(\boldsymbol{r}_2 \times \boldsymbol{\Omega}_2 + \boldsymbol{v}_2)\right], \quad (11)$$

where $\boldsymbol{\Omega}_i$ is the rotation angular velocity of the ith planet, for $i = 1, 2$. It is worth noting that Mignard's force is given by a closed formula and, therefore, is valid for any value of eccentricity.[3] Δt_i is the time lag and can be interpreted as a delay in the deformation of the tidally affected body due to its internal viscosity.

The time lag is related to the dissipation function (Q) of the deformed planet, which is a quantity used in the study of the tidal evolution of extra-solar planets. However, in many classical theories, the tidal potential appears written as a function of phase lags (ε_j) of tidal waves, introduced in each periodic term in order to consider the effect of viscosity (Darwin 1880; Kaula 1964; Ferraz-Mello et al. 2008). In fact, the expansion of equations (10)–(11) leads to the same forces used in Darwin's theory when the phase lags of the tide components are assumed proportional to their frequencies (the so-called linear model): $\varepsilon_j = \nu_j\Delta t$, with the same Δt for all j-frequencies. For small lags, Q can be associated with the phase lag of the tidal wave through $\varepsilon = 1/Q$ [see Efroimsky & Lainey (2007) and Efroimsky & Williams (2009) for a complete discussion]. For planets in stationary or synchronous rotation, the tidal evolution is well described by the phase lag corresponding to the frequency n (annual tide; see Ferraz-Mello et al. 2008). Thus, in the linear model we have $1/Q \simeq n\Delta t$ or, using a modified definition which absorbs the Love number, $Q' \equiv 3Q/2k$, we obtain $k\Delta t = 3/(2Q'n)$ (see Leconte et al. 2010).

3.2 Application 1: CoRoT-7 planets

We numerically investigate the recently discovered CoRoT-7 planetary system, which is composed of two short-period planets orbiting a central star. The star, CoRoT-7, is G9V with mass $m_0 = 0.93\,\text{M}_\odot$, radius $R_0 = 0.87\,\text{R}_\odot$ and age of 1.2–2.3 Gyr (Bruntt et al. 2010). The inner planet, CoRoT-7b, and the outer planet, CoRoT-7c, are assumed to have the masses given in Ferraz-Mello et al. (2011), $m_1 = 8.0\,m_\oplus$ and $m_2 = 13.6\,m_\oplus$, respectively. The radius of CoRoT-7c is not known. We adopted values of Q' and mean density consistent with a rocky terrestrial planet. Their orbital periods are $P_{1\,\text{orb}} = 0.854$ and $P_{2\,\text{orb}} = 3.698$ d (Léger et al. 2009; Queloz et al. 2009). CoRoT-7b is the third exoplanet with the shortest orbital period discovered up to the present date.

The adopted physical and orbital parameters of the system are listed in Table 1. As we will show, in the current configuration of the system, both orbits must be circular. We emphasize that the masses of the CoRoT-7 planets satisfy the relation $m_1/m_2 < 1$. Choosing $Q'_1 = Q'_2 = 100$ (a typical value for terrestrial planets) and using

---

[3] Note, however, that, for a more accurate description, a large number of harmonics in the expansion of the tidal potential should be considered when the star–planet distance is small enough (see Taylor & Margot 2010).

current values of semimajor axes, we obtain $k_1\Delta t_1 = 3$ min and $k_2\Delta t_2 = 12$ min. A scaling factor is often used in the numerical simulations in order to accelerate the process of tidal evolution. In the simulations reported in this paper, we did not use a scaling factor. We also assume that the inclinations of both orbital planes with respect to the reference plane are zero.

The next step to perform the simulation is the choice of the initial configuration of the CoRoT-7 system. (It should be emphasized that, since we are studying a dissipative process, we cannot use a simple backward simulation for that sake). The choice is arbitrary, but it can be constrained by some considerations. We assume that the planets have experienced an orbital decay due to tidal effects; thus its past location must be more distant from the central star than the current one. Finally, as will be discussed in Section 4, the angular momentum of the system can be considered as invariable during the evolution of the system under the interplay of the gravitational and tidal forces. Gathering this information, we assume the following initial values for the orbital elements: $e_{1\,ini} = 0$, $e_{2\,ini} = 0.2$, $a_{1\,ini} = 0.0188$ au and $a_{2\,ini} = 0.0462$ au.

Figs 2 and 3 show the result of a numerical integration of equations (7) and (8) using the RA15 code (Everhart 1985). It shows the orbital decay and circularization of the orbits due to tidal effects. The inner planet eccentricity initially undergoes large variations, but, after a short time of damped oscillations, it reaches a quasi-equilibrium value (Mardling 2007, see Section 3.2.1). After relaxation, e_1 decreases smoothly to reach near-circularization in about 7 Myr. The eccentricity of the outer planet is also damped and a pair of circular orbits is obtained as a final configuration of the system.
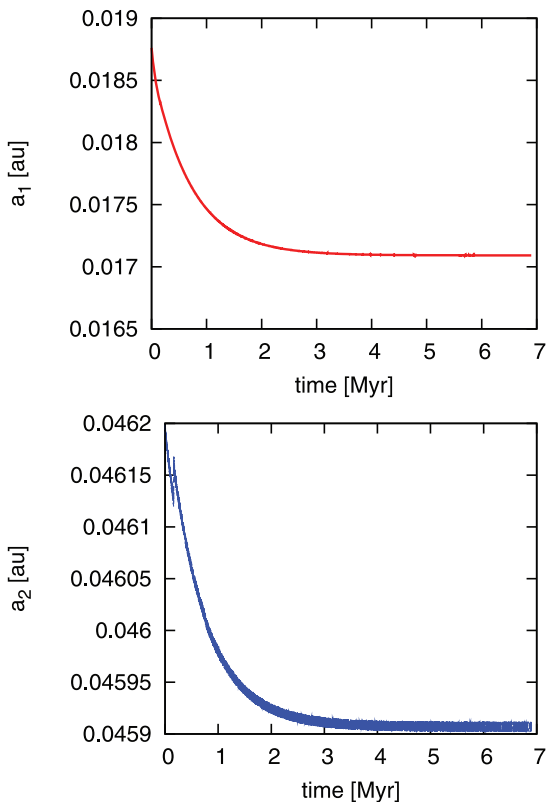

Figure 2. Time variation of semimajor axes for the planets of the CoRoT-7 system. The excitation of e_1 enables the orbital decay of CoRoT-7b due to tides on the planet raised by the star. CoRoT-7c also migrates due to tides but with a slower rate, resulting in a divergent migration between the planets.
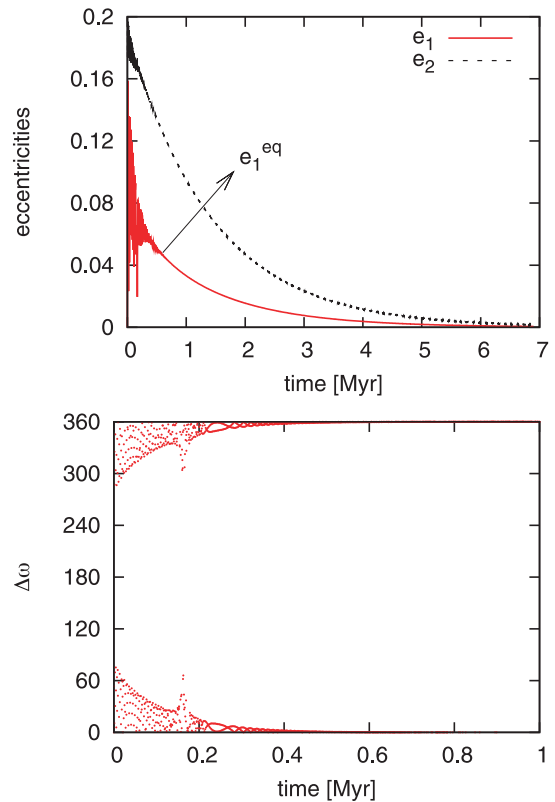

Figure 3. Time variation of eccentricities and $\Delta\varpi$ (in degrees) for the planets of the CoRoT-7 system. The eccentricity of the initial inner circular orbit is excited by the outer companion. Tides on the inner planet circularize its orbit in approximately 7 Myr. The eccentricity of the outer orbit is also damped because of the total angular momentum conservation (see Section 4). At the end of the simulation, a state of double circularization is obtained (see the text for discussion).

The excitation of e_1 activates the orbital decay of the inner planet, which requires a non-circular orbit according to equation (1) (with $\hat{s} = 0$, because we are not considering the contribution of stellar tides in our simulations). The migration of CoRoT-7b towards the star occurs until the circularization of its orbit. Meanwhile, a_2 also decreases (and is only weakly affected when the 4/1 mean-motion resonance is crossed). However, when equations (10)–(11) are expanded up to the third order in eccentricities (see Ferraz-Mello et al. 2008), the ratio of forces on CoRoT-7b and CoRoT-7c is approximately 16, indicating a more intense migration of the inner planet.

The bottom panel of Fig. 3 shows the time variation of the secular angle $\Delta\varpi \equiv \varpi_1 - \varpi_2$, where ϖ means longitude of pericentre. Initially, $\Delta\varpi$ oscillates around $\Delta\varpi = 0°$ with large amplitude; this stage of the evolution corresponds to the damped oscillations of the planetary eccentricities. Reaching the relaxed state, in which the system oscillates with amplitudes close to zero, the oscillation amplitude of the secular angle also tends to zero.

It is worth mentioning that, due to the divergent migration between the planets, capture in mean-motion resonance is not possible.

3.2.1 The short-time evolution of the eccentricity of CoRoT-7b

Fig. 3 shows that, approximately at $t = 0.5$ Myr, the amplitudes of oscillation of the eccentricities are damped and the variation becomes smooth. This situation is called quasi-equilibrium. Mardling
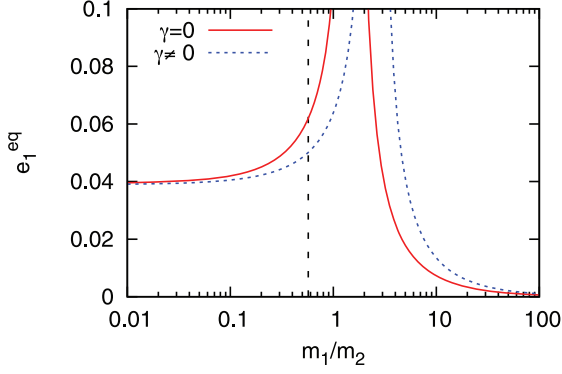
Figure 4. Quasi-equilibrium e_1^{eq} given by equation (12), as a function of the mass ratio. The vertical dashed line corresponds to the mass ratio of the CoRoT-7 system. The curves show the cases with and without general relativity.

(2007) derived an expression to compute the quasi-equilibrium value of the inner planet eccentricity, e_1^{eq}, using the Legendre expansion of the disturbing function, up to the fourth order in a_1/a_2. It is given by

$$e_1^{\mathrm{eq}} = \frac{(5/4)(a_1/a_2)e_2\varepsilon_2^{-2}}{\left| 1 - \sqrt{a_1/a_2}(m_1/m_2)\varepsilon_2^{-1} + \gamma\varepsilon_2^3 \right|}, \qquad (12)$$

where $\varepsilon_2 \equiv \sqrt{1 - e_2^2}$ and $\gamma \equiv 4(n_1 a_1/c)^2(m_0/m_2)(a_2/a_1)^3$.

Fig. 4 shows the variation of e_1^{eq} given by equation (12), for CoRoT-7, as a function of m_1/m_2. The relevant value of e_2 which should be used is the one when e_1^{eq} is reached. In addition, the condition (12) was obtained under the assumption that semimajor axes are constants. We show the cases with ($\gamma \neq 0$) and without ($\gamma = 0$) the contribution of general relativity. The inclusion of $\gamma \neq 0$ reduces the value of e_1^{eq}. Hence, since the mean rate of orbital decay is proportional to e_1^2, the omission of the relativistic potential can result in an underestimation of the circularization and orbital decay time-scales. Mardling & Lin (2004) also showed that the inclusion of the relativistic potential is very important when the planet approaches the star.

3.2.2 The long-time evolution of the eccentricity of CoRoT-7c

Our numerical simulation has shown that the eccentricity of the outer planet is strongly affected during the orbital decay (see Fig. 2, top panel). However, the source of e_2 damping is not the direct action of tides on the outer planet since, as we have already shown, the magnitude of the tidal force on CoRoT-7c is much smaller than the corresponding force on CoRoT-7b.[4]

Mardling (2007) also studied the long-term variation of the outer planet eccentricity and provided an expression to calculate the e_2 damping:

$$\dot{e}_2 = -\frac{\lambda}{\tau_{\mathrm{circ}}} \frac{e_2}{F(e_2)}, \qquad (13)$$

where τ_{circ} is the circularization time-scale of the inner orbit in the single-planet case [i.e. $e_1/\dot{e}_1$, where $\dot{e}_1$ is given by equation (2)];

---

[4] One can take an idea about which is the contribution of tides raised in the outer planet to the circularization process of its orbit. For that sake, we note that the ratio between the circularization time-scales associated with the direct tidal interaction with the star and the one given by equation (13) is of the order of $(a_2/a_1)^4 \gg 1$.
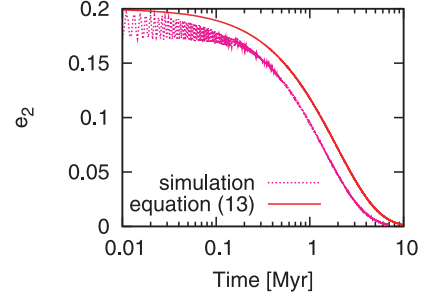
Figure 5. Time variation of e_2 in the CoRoT-7 system. The comparison is done between the integration of equation (13) and the result of the numerical simulation (see the text for more discussion).

$\lambda \equiv (25/16)(m_1/m_2)(a_1/a_2)^{5/2}$ and $F(e_2) \equiv \varepsilon_2^3(1 - \alpha\,\varepsilon_2^{-1} + \gamma\,\varepsilon_2^3)^2$, with $\alpha \equiv (m_1/m_2)(a_1/a_2)^{1/2}$.

The comparison between the integration of equation (13) and the result of the simulation of exact equations of motion (7) and (8) is shown in Fig. 5. The difference between both results may arise from the fact that to obtain equation (13) it is explicitly assumed that semimajor axes are constant (see Mardling 2007).[5] In Section 3.3, we will show that the disagreement increases in a system for which $m_1/m_2 \ll 1$.

We note that, according to equation (13), the rate of e_2 damping decreases with m_2/m_1, enabling a non-circular outer orbit to be maintained over long times. In addition, e_1^{eq} increases with e_2 as equation (12) indicates. Hence, since the mean rate of the orbital decay is proportional to e_1^2, a significant inner orbital shrinkage can occur for large m_2/m_1 (see the next section).

3.2.3 The rotation of CoRoT-7b and CoRoT-7c

The tidal force produces a torque that directly affects the rotation evolution of the deformed bodies in such a way that $C_1\dot{\boldsymbol{\Omega}}_1 = \boldsymbol{r}_1 \times \boldsymbol{f}$ and $C_2\dot{\boldsymbol{\Omega}}_2 = \boldsymbol{r}_2 \times \boldsymbol{g}$. Thus,

$$C_i\dot{\boldsymbol{\Omega}}_i = -3k_i\Delta t_i \frac{Gm_0^2 R_i^5}{r_i^8}\left[-r_i^2\boldsymbol{\Omega}_i + \boldsymbol{r}_i \times \boldsymbol{v}_i\right], \qquad (14)$$

where C_i is the polar moment of inertia of the ith planet.

To obtain the time evolution of the angular velocity Ω_i, the above equations ($i = 1, 2$) were integrated simultaneously with the equations of motion (7)–(8). The result of the integration is shown in Fig. 6. The rotation periods, defined as $P_{i\,\mathrm{rot}} = 2\pi/\Omega_i$, reach stationary values, which, up to second order in e_i, are given by $P_{i\,\mathrm{rot}} = P_{i\,\mathrm{orb}}/(1 + 6e_i^2)$ (Hut 1981; also see Ferraz-Mello et al. 2008; Correia, Levrard & Laskar 2008). In the same figure, we also plot the orbital periods defined as $P_{i\,\mathrm{orb}} = 2\pi/n_i$, which decrease as a consequence of the orbital decay. The synchronization between the orbital motions and the rotation of the planets occurs when $\Omega_i = n_i$ or $P_{i\,\mathrm{rot}} = P_{i\,\mathrm{orb}}$. In Fig. 6 we can observe that this condition is only reached after the circularization of the planet orbits.

---

[5] We stress that equation (13) gives an estimate for the damping time-scale of e_2 [the full expression is given in equation (57) of Mardling 2007]. However, it is shown in that work that the approximate solution (13) underestimates the time-scale on which e_2 evolves. Hence, the difference between analytical and numerical results would be even large if the full expression were used.
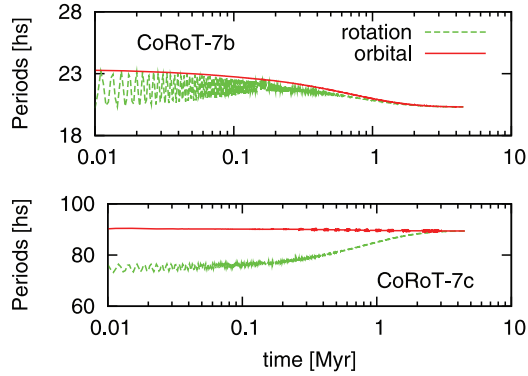
Figure 6. Time variation of the rotation and orbital periods of CoRoT-7 planets. Synchronization is reached as the doubly circular state approaches.

Table 2. Orbital elements and physical data corresponding to a hypothetical Sun–super-Earth–Jupiter system. The value of R_1 was computed assuming a terrestrial mean density.

Body	m_i	R_i	a_i (au)	e_i	Q'_i
0	$1\,\mathrm{M_\odot}$	$1\,\mathrm{R_\odot}$	–	–	–
1	$5\,m_\oplus$	$5^{1/3}R_\oplus$	0.04	0.1	100
2	$1\,m_\mathrm{J}$	–	0.1	0.1	–

3.3 Application 2: super-Earth with a giant companion

In this section, we investigate the tidal evolution of a system in which the inner planet is much smaller than the outer one. We chose a fictitious system composed of a super-Earth and a Jupiter-like outer companion, with masses $m_1 = 5\,m_\oplus$ and $m_2 = 1\,m_\mathrm{J}$, respectively (m_J is the mass of Jupiter). Note that $m_1/m_2 \simeq 0.0157 \ll 1$. The initial configuration and physical parameters of this hypothetical system are listed in Table 2, in which the values of semimajor axes correspond to orbital periods of 2.92 and 11.6 d. The large orbital period of the outer planet, in addition to the large Q-value for Jupiter-like planets, enables us to neglect the tides on the outer companion. Moreover, as shown in Fig. 7 for the considered system, the contribution of the relativistic potential is also negligible. Here, we also assume zero inclinations. In addition, the calculation of $k_1 \Delta t_1 = 3/(2Q'_1 n_1)$ with $Q'_1 = 100$ results in $k_1 \Delta t_1 = 10$ min.

3.3.1 Short-time evolution (50 Myr)

Fig. 8 shows the time evolution of the inner planet semimajor axis (solid curve in the top panel) and two eccentricities (bottom panel) over the first 50 Myr. Due to the large mass of the outer planet,
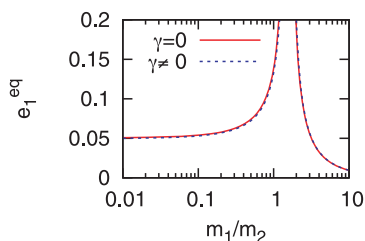

Figure 7. Quasi-equilibrium e_1^{eq} in the second application, given by equation (12), as a function of the mass ratio. The contribution of general relativity does not affect the value of e_1^{eq} and thus can be neglected.
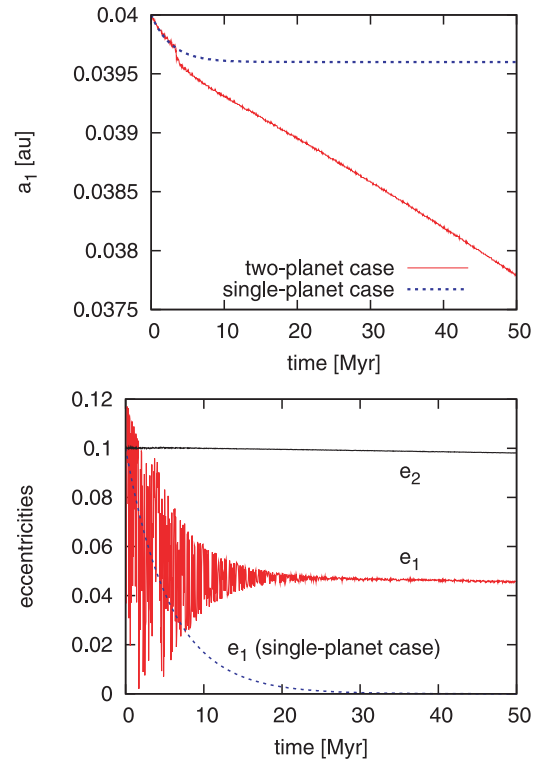

Figure 8. Time variations of orbital elements in the case $m_1/m_2 \ll 1$ (cf. Table 2). The evolution in the case in which the super-Earth is the only planet is also shown. The inner orbit reaches a quasi-equilibrium value in 25 Myr, retarding the orbital circularization and enhancing the orbital decay.

e_2 is almost constant over the time interval shown in the figure (see equation 13). In contrast, e_1 initially suffers large oscillations which are quickly damped to the quasi-equilibrium value. On the same graph, we plot the variation of e_1 in the case of a single-planet system, when the interactions with one outer planet do not exist. Comparing the two cases, we note that the presence of the outer companion delays the circularization of the inner planet orbit (see Fig. 9). As a consequence, the presence of the second planet leads to a faster decay of the inner planet orbit. [In the single-planet case, the semimajor axis a_1 decreases only slightly and reaches a final constant value (0.0396 au) after total circularization.][6]

3.3.2 Long-time evolution (300 Myr)

Fig. 9 shows the time variation of the planet semimajor axes (top panel) and the eccentricities (bottom panel) over 300 Myr. After e_1^{eq} is reached, the inner planet eccentricity decreases smoothly to very small values. The outer eccentricity follows the evolution of the inner one and, at the end of the simulation, about $\simeq 0.25$ Gyr, a pair of circular orbits is obtained. When the time approximates to 0.12 Gyr, e_1 is strongly excited due to the passage of the system through the 5/1 mean-motion resonance but, immediately after that, it is damped to its previous value.

The orbital decay of the inner planet occurs until the total circularization of its orbit (see the top panel in Fig. 9). Note that the final position of the super-Earth is close to the Roche limit $a_{\mathrm{Roche}} = (R_1/0.462)(m_0/m_1)^{1/3}$ (Faber, Rasio & Willems 2005),

---

[6] This value can be obtained using equation (6) with $e = 0$, $e_{\mathrm{ini}} = 0.1$ and $a_{\mathrm{ini}} = 0.04$ au.
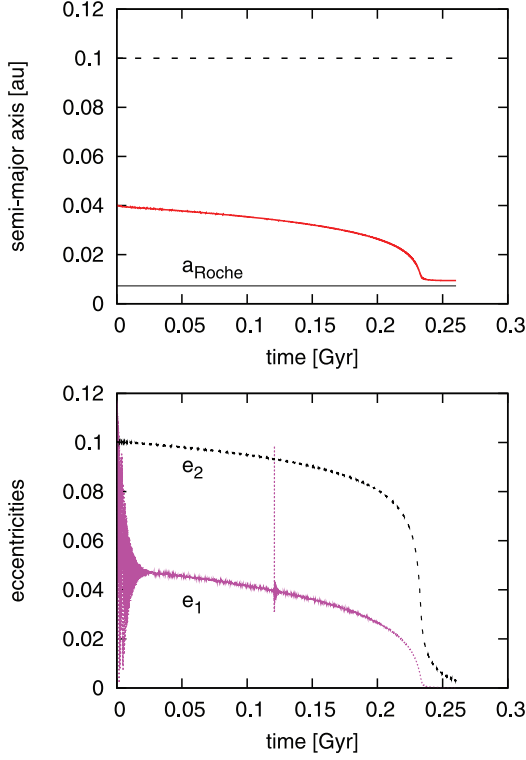
Figure 9. Long-term evolution of semimajor axes and eccentricities in a Sun–super-Earth–Jupiter system. Due to the orbital decay, the final position of the inner planet is close to the Roche limit. The value of e_1 is damped to zero and the outer orbit is also circularized.

which gives $a_{\text{Roche}} = 0.0064$ au. The outer planet semimajor axis does not vary in the considered time interval.

In Fig. 10, we compare the damping of e_2 resulting from the numerical simulation (dashed line) and that obtained through the integration of equation (13) of Mardling's model (solid line). The results are very different, indicating that equation (13) is not a good approximation to compute the decrease of e_2 in the case of the massive outer companion. The discrepancy can be understood taking into account that, for this particular system, there is a significant orbital decay due to tides on the inner planet, while equation (13) was obtained assuming λ and α as constants, i.e. constant semimajor axes (Mardling 2007). Thus, it is shown that the process of outer planet circularization is accelerated in the case of significant
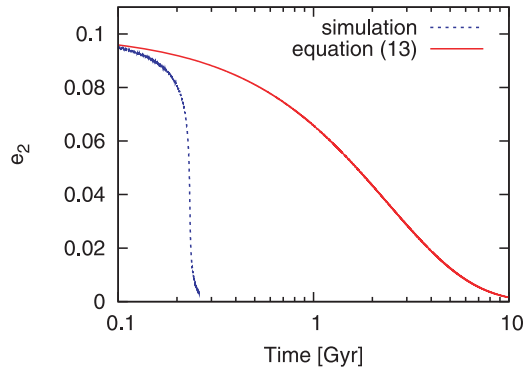

Figure 10. Time variation of e_2 in a Sun–super-Earth–Jupiter system. The comparison is done between the integration of equation (13) and the result of numerical simulation (see the text for more discussion).

orbital decay of the inner planet, if compared with the result of equation (13).

4 CONSERVATION OF THE ANGULAR MOMENTUM

Many dynamical features of the planet evolution shown in the previous sections can be explained considering the conservation of the angular momentum of the system. The total angular momentum of the three-body system in the astrocentric reference is the vectorial sum of the orbital momenta of the planets, L_i^{orb} ($i = 1, 2$), and the rotational momenta of the planets and star, L_i^{rot} ($i = 0, 1, 2$).

If r_i is the astrocentrical position of the ith planet, the orbital component of the angular momentum is given by

$$L_{\text{orb}} = \sum_{i=1}^{2} m_i r_i \times \dot{r}_i - \frac{1}{M} \sum_{i=1}^{2} m_i r_i \times \sum_{i=1}^{2} m_i \dot{r}_i, \quad (15)$$

where $M \equiv \sum_{i=0}^{2} m_i$. Note that the second term of equation (15) appears due to the use of the astrocentric reference frame. This term is of second order in masses and, assuming $m_i \ll m_0$, can be neglected. Moreover, $r_i \times \dot{r}_i = \sqrt{G(m_0 + m_i)a_i(1 - e_i^2)}\,\hat{k}$, where $\hat{k}$ is a unitary vector normal to orbital planes. Hence

$$L_{\text{orb}} \simeq \sum_{i=1}^{2} m_i' \sqrt{a_i \left(1 - e_i^2\right)}\,\hat{k}, \quad (16)$$

where $m_i' \equiv m_i \sqrt{Gm_0}$.

The rotation component of the angular momentum is given by

$$L_i^{\text{rot}} = \sum_{i=0}^{2} C_i \Omega_i,$$

where C_i are the moment of inertia with respect to the axes of rotation and Ω_i are the angular velocities of rotation, for $i = 0, 1, 2$. Because we account only for the planetary tides on the planets, Ω_1 and Ω_2 vary with time, while Ω_0 is constant.

We can show that for planets, $L_i^{\text{rot}} \ll L_i^{\text{orb}}$; thus, the contribution of the rotational component to the total angular momentum can be neglected. Indeed, using Kepler's third law, we have $L_i^{\text{rot}}/L_i^{\text{orb}} = \xi_i(R_i/a_i)^2(\Omega_i/n_i)$, where we have introduced $C_i = \xi_i m_i R_i^2$, with $0 < \xi_i \le 2/5$. In the case of the quasi-synchronous planet discussed in Section 3.2.3, when $\Omega_i \simeq n_i$, this ratio is small, of the order of $(R_i/a_i)^2$.

In contrast, for the star, the quantity $L_0^{\text{rot}}/L_i^{\text{orb}} = \xi_0(m_0/m_i)(R_0/a_i)^2(\Omega_0/n_i)$ is close to unity, when we consider close-in planets and a slow-rotating star, for which the condition $\Omega_0 \ll n_i$ is satisfied. Hence, the total angular momentum of the system can be approximately written as

$$L \simeq \left(m_1' \sqrt{a_1 \left(1 - e_1^2\right)} + m_2' \sqrt{a_2 \left(1 - e_2^2\right)} + C_0\Omega_0\right)\hat{k}. \quad (17)$$

It should be noted that some quantity of angular momentum is removed due to the orbital decay of the inner planet. Thus, according to the above equation, for small e_1, the eccentricity of the outer planet would be damped in order to preserve the angular momentum conservation.

4.1 The orbital decay

As a consequence of the total angular momentum conservation, we can obtain the minimal possible value for a_1/a_2 during the orbital decay, knowing that this minimum value should be achieved

once orbital circularization is reached. Imposing $e_1 = e_2 = 0$ in equation (17) we obtain

$$\frac{a_{1\min}}{a_2} = (L' - 1)^2 \left(\frac{m_2}{m_1}\right)^2, \qquad (18)$$

where $L' \equiv (L - C_0\Omega_0)/m'_2\sqrt{a_2}$ and $m'_2/m'_1 \simeq m_2/m_1$. For those cases in which tides on the outer planet can be neglected, a_2 and thus L' are constants of the problem. Applying equation (18) to the super-Earth–Jupiter system we obtain $a_{1\min}/a_2 \simeq 0.096$, reproducing the corresponding result of the numerical simulation. Hence, it is worth noting that the final position of the inner planet can be obtained from the analysis of the angular momentum conservation, as given by equation (18).

Equation (18) allows us to investigate the variation of $a_{1\min}/a_2$ for several mass ratios. However, we note that there is also an implicit dependence on m_2/m_1 through L', which is not shown in equation (18). Hence, in order to express the full dependence we define two constants, namely $\kappa_1 \equiv \sqrt{(a_{1\,\mathrm{ini}}/a_{2\,\mathrm{ini}})(1 - e_{1\,\mathrm{ini}}^2)}$ and $\kappa_2 \equiv \sqrt{1 - e_{2\,\mathrm{ini}}^2}$. Using the definition of L' and replacing it into equation (18), we obtain

$$a_{1\min} = a_2 \left[(\kappa_2 - 1)\frac{m_2}{m_1} + \kappa_1\right]^2. \qquad (19)$$

Fig. 11 shows the variation of $a_{1\min}$ with the mass ratio m_2/m_1 according to equation (19), where we have used initial values of the orbital elements listed in Table 2. We see that, for fixed initial values of the elements, the inner planet will come closer to the star for high-mass companions. Therefore, as discussed in Section 3.2.2, the orbital decay of the inner planet is enhanced.

For the sake of completeness, we show in the bottom panel of Fig. 11 the result for $m_2/m_1 < 1$, which is the case of a more massive inner planet. Note that the orbital decay is very weak, supporting the assumptions made in Mardling (2007) of constant semimajor axes in the case of slow-mass outer companions.
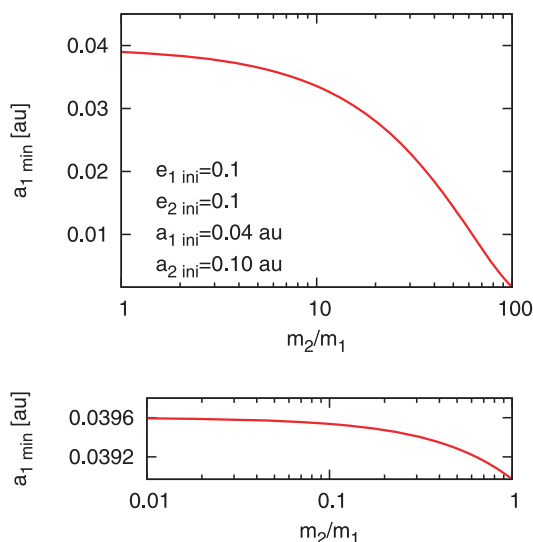

Figure 11. A plot of equation (19) showing the dependence of the minimum value of the inner planet semimajor axis with m_2/m_1. The initial elements of Table 2 were used to compute κ_1 and κ_2. The case of a more massive inner planet is shown in the bottom panel.

5 EVOLUTIONARY ROUTES IN THE PHASE SPACE

In this section, we will show that evolutionary routes of the migrating system are traced by stationary solutions of the conservative secular problem. For this task, we explore the secular dynamics of the planar two-planet system, described in detail in Michtchenko & Ferraz-Mello (2001) and Michtchenko & Malhotra (2004).

In the context of the Hamiltonian formalism, the stationary values are defined by the secular Hamiltonian function, in which the fast-period terms, involving arguments with combinations of mean longitudes, are removed by first-order averaging. In this case, the secular problem of coplanar two-planet systems is reduced to one degree of freedom. Regarding the angle $\Delta\varpi$, the stationary solutions are restricted to $\Delta\varpi = 0°$ and $\Delta\varpi = 180°$, which correspond to Mode I and Mode II solutions, respectively. In addition, the stationary values of eccentricities for these modes are $e_{i\mathrm{I}}^*$ and $e_{i\mathrm{II}}^*$, for $i = 1, 2$. Periodic solutions of the secular system are circulations or oscillations around Modes I or II and the stationary solution can be represented by a point in the plane of eccentricities. The position of this point in the phase space depends on the parameters of the secular problem, namely angular momentum and semimajor axis ratio.

To understand how the stationary solutions are affected by the introduction of dissipative forces on the system, we will assume that the dissipation is very slow. This means that the dissipation rate is much smaller than the characteristic time of the secular system, which is the proper period of the secular angle $\Delta\varpi$. Under this assumption, the motion of the pair of planets is nearly conservative and, for very short time intervals, it can be described by the classical secular theory.

For the sake of simplicity, let us consider that periodic solutions are oscillations around Mode I. When the tidal effects are taken into account, the semimajor axis of the inner planet decreases slowly. Since the semimajor axis ratio is changed, the position of the equilibrium $(e_{1\mathrm{I}}^*, e_{2\mathrm{I}}^*)$ in the phase space will be also changed, in order to preserve the total angular momentum of the system. In such a way, the system oscillates around a centre whose position in the phase space changes slowly due to dissipation.

Assuming continuous values of the inner semimajor axis, we obtain the equilibria $(e_{1\mathrm{I}}^*, e_{2\mathrm{I}}^*)$, for all possible values of a_1. A curve in the space (e_1, e_2), which is composed of successive equilibrium points, is a locus of stationary solutions in the space of eccentricities, and we refer to it as LSE. By definition, all solutions in the LSE curve have the same value of angular momentum.

Fig. 12 illustrates the LSE curve for Mode I in the case of the CoRoT-7 planets,[7] comparing with the curve resulting from numerical simulation of the system. For the sake of simplicity, we do not include the relativistic potential in the analysis of mean equations. The initial conditions for the numerical integration were chosen as $\Delta\varpi = 0$, $e_1 = 0$ and $e_2 = 0.2$. Initially, the eccentricities oscillate rapidly with decreasing amplitudes around an equilibrium which slides slowly along the LSE curve. When $e_1 \simeq 0.05$ and $e_2 \simeq 0.08$, the amplitude of oscillation becomes close to zero and the solution is almost coincident with the LSE curve, until the system reaches total orbital circularization.

Detailed discussion about the secular dynamics of non-conservative two-planet systems can be found in Michtchenko & Rodríguez (2011).

---

[7] We have seen in Section 3.2 that the angle $\Delta\varpi$ oscillates with almost zero amplitude around $\Delta\varpi = 0°$, indicating motion around Mode I.
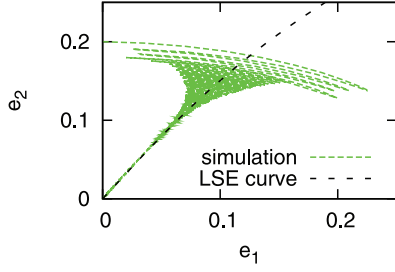
Figure 12. Comparison between the computation of the LSE curve and the result of numerical simulation for the CoRoT-7 system (without the contribution of the relativistic potential). After the angle $\Delta\varpi$ is close to $0°$ (Mode I), both curves are almost coincident.

6 THE ROLE OF STELLAR TIDES

In this section, we evaluate the time required for CoRoT-7 planets to reach the Roche limit with the star. As seen in Section 2, in the case of small-mass planets, the contribution of tides raised by the planet on the star can be neglected if compared with the contribution of tides raised by the star on the planet. However, we know that after orbital circularization, the stellar tide is the only source of the orbital decay. Thus, due to the current orbital configuration of the CoRoT-7 system, with two circular orbits, only the stellar tides could produce the orbital decay.

We define the mean lifetime of CoRoT-7b as the time for which the Roche limit is reached, starting with $a_1 = a_{1\,\text{current}} = 0.017$ au. According to equation (1) with $\hat{p} = 0$, $e_1 = 0$ and in the limit $m_1 \ll m_0$, the mean rate of semimajor axis variation is

$$\langle \dot{a}_1 \rangle = -\frac{3\sqrt{Gm_0}}{a_1^{11/2}} \frac{k_0}{Q_0} \frac{m_1}{m_0} R_0^5. \tag{20}$$

Equation (20) can be integrated as

$$\int_{a_{1\,\text{current}}}^{a_{\text{Roche}}} \mathrm{d}a_1 \, a_1^{11/2} = -\mathcal{K}\, \tau_{a_1}, \tag{21}$$

where $\mathcal{K} \equiv 3\sqrt{Gm_0}(k_0/Q_0)(m_1/m_0)R_0^5$, whereas τ_{a_1} is the mean lifetime of CoRoT-7b and $a_{\text{Roche}} = 0.0049$ au ($\simeq 1.2\,R_0$). Solving for τ_{a_1}, we obtain

$$\tau_{a_1} = \frac{2}{39} \frac{\left(a_{1\,\text{current}}^{13/2} - a_{\text{Roche}}^{13/2}\right)}{\sqrt{Gm_0}R_0^5} \frac{Q_0}{k_0} \frac{m_0}{m_1}. \tag{22}$$

Fig. 13 shows the variation of τ_{a_1} as a function of k_0/Q_0 according to equation (22). It is easy to see that the mean lifetime of
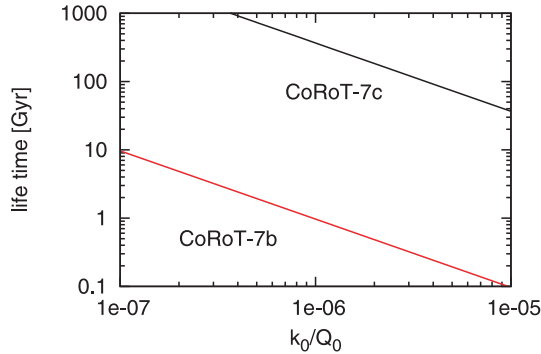

Figure 13. The mean lifetime τ_{a_1} of CoRoT-7 planets due to stellar tides in the function of the dissipation on the star. For $k_0/Q_0 = 10^{-6}$, $\tau_{a_1} = 0.97$ Gyr and $\tau_{a_2} = 367$ Gyr.

CoRoT-7b is small for high values of k_0/Q_0. On the other hand, τ_{a_1} increases when the energy within the star is not efficiently dissipated (small k_0/Q_0). For a typical value of $k_0/Q_0 = 10^{-6}$, we obtain $\tau_{a_1} = 0.97$ Gyr (see also Jackson, Barnes & Greenberg 2009). If the same analysis is done for CoRoT-7c, we obtain $a_{\text{Roche}} = 0.0062$ au ($\simeq 1.5\,R_0$) and $\tau_{a_1} = 367$ Gyr, indicating that CoRoT-7c should not be destroyed by tides within the lifetime of the star.

7 DISCUSSION AND CONCLUSIONS

In this work we have investigated the tidal evolution of super-Earth planets with exterior companions. Previous works have already discussed that problem, giving special attention to the case of a more massive inner planet. In Mardling (2007), explicit equations were obtained giving the variation of eccentricities in the context of constant semimajor axes (see equations 12 and 13). Here, we centre attention on the case of a more massive outer companion.

Through an approach in which the exact equations of motion are numerically solved, we have shown that the super-Earth orbital decay is accompanied by orbital circularization of both planets. In addition, we show that the rate of e_2 damping is small for large values of m_2/m_1, enabling a non-circular outer orbit to be sustained for longer times. Thus, as e_1^{eq} increases with e_2, a significant inner orbital decay can occur for large m_2/m_1, since its mean rate is proportional to e_1^2.

As a real application of the tidal evolution of a super-Earth accompanied by a more massive outer planet, we investigated the CoRoT-7 two-planet system. We have shown that, starting from an initial circular orbit, e_1 is excited, enabling the activation of the orbital decay of CoRoT-7b (which requires a non-zero value of e_1). The equilibrium value of e_1 is quickly damped by tides on the planet and a strong decrease in a_1 is observed in the short-term tidal evolution.

In addition, the long-term tidal evolution has shown that the current orbital configuration of the system is achieved, including the double-circularization state of CoRoT-7 planets. After circularization, the migration towards the star continues due to the action of stellar tides. We have shown that CoRoT-7b can reach the Roche limit in approximately 1 Gyr for $k_1/Q_1 = 10^{-6}$ (see also Jackson et al. 2009).

The study of stationary solutions of mean equations is useful to better understand the secular dynamics in the space $e_i \cos \Delta\varpi - e_i \sin \Delta\varpi$. The periodic solutions around Mode I (aligned pericentres) and Mode II (anti-aligned pericentres) may be easily identified in the conservative case. In addition, the analysis can be extended to the case in which dissipation is included. It is possible to construct a curve in the space of eccentricities composed of successive stationary solutions, which are obtained one by one through the same technique used in the conservative case. We have shown that the result of the numerical simulation of exact equations for CoRoT-7 planets is in good agreement with the curve of stationary solutions of mean equations of motion.

Future studies involving the dynamical evolution of a two-planet pair including tidal dissipation will help us to investigate the past history of the CoRoT-7 system (i.e. formation and the subsequent evolution). This may bring more information about how the current orbital configuration of the system was achieved.

As an example in which $m_1/m_2 \ll 1$, we have also investigated the tidal evolution of a Sun–super-Earth–Jupiter-like system. The results of the numerical simulation have shown that e_2 is not well described by integration of the simple model represented by equation (13), which describes the time variation of e_2 in the long-term

evolution. We have shown that the doubly circular state is accelerated when there is a significant orbital migration of the inner planet, showing that the final configuration of the system is affected by the shrinking of the inner orbit.

A simple analysis based on the angular momentum conservation shows that it is possible to predict the final value of the inner planet semimajor axis, provided the semimajor axis of the outer planet is fixed.

ACKNOWLEDGMENTS

REFERENCES

Barnes R., Raymond S. N., Greenberg R., Jackson B., Kaib N. A., 2010, AJ, 709, L95
Beutler G., 2005, Methods of Celestial Mechanics, Vol. I. Springer, Berlin
Bruntt H. et al., 2010, A&A, 519, A51
Correia A. C. M., Levrard B., Laskar J., 2008, A&A, 488, L63
Darwin G. H., 1880, Philos. Trans., 171, 713 (repr. Scientific Papers, Cambridge, Vol. II, 1908)
Dobbs-Dixon I., Lin D. N. C., Mardling R. A., 2004, AJ, 610, 464
Efroimsky M., Lainey V., 2007, J. Geophys. Res. (Planets), 112, 12003
Efroimsky M., Williams J. G., 2009, Celest. Mech. Dynamical Astron., 104, 257
Everhart E., 1985, in Carusi A., Valsecchi G. B., eds, Dynamics of Comets: Their Origin and Evolution. Reidel, Dordrecht, p. 185
Faber J. A., Rasio F. A., Willems B., 2005, Icarus, 175, 248
Ferraz-Mello S., Rodríguez A., Hussmann H., 2008, Celest. Mech. Dynamical Astron., 101, 171 [Erratum: 2009, Celest. Mech. Dynamical Astron., 104, 319]
Ferraz-Mello S., Tadeu M., Michtchenko T. A., Beaugé C., Rodríguez A., 2011, preprint (arXiv:1011.2144)
Fortney J. J., Marley M. S., Barnes J. W., 2007, ApJ, 659, 1661
Greenberg R., Van Laerhoven C., 2011, ApJ, in press (arXiv:1103.2794)
Hut P., 1981, A&A, 99, 126
Jackson B., Greenberg R., Barnes R., 2008, ApJ, 678, 1396
Jackson B., Barnes R., Greenberg R., 2009, ApJ, 698, 1357
Kaula W. M., 1964, Rev. Geophys. Space Phys., 2, 661
Leconte J., Chabrier G., Baraffe I., Levrard B., 2010, A&A, 516, L64
Léger A. et al., 2009, A&A, 506, 287
Mardling R. A., 2007, MNRAS, 382, 1768
Mardling R. A., 2010, MNRAS, 407, 1048
Mardling R. A., Lin D. N. C., 2004, ApJ, 614, 955
Michtchenko T. A., Ferraz-Mello S., 2001, Icarus, 149, 357
Michtchenko T. A., Malhotra R., 2004, Icarus, 168, 237
Michtchenko T. A., Rodríguez A., 2011, MNRAS, in press (arXiv:1103.5485, doi:10.1111/j.1365-2966.2011.18857.x)
Mignard F., 1979, Moon Planets, 20, 301
Queloz D. et al., 2009, A&A, 506, 303
Rodríguez A., Ferraz-Mello S., 2010, EAS Publ. Series, 42, 411
Taylor P. A., Margot J. L., 2010, Celest. Mech. Dynamical Astron., 108, 315
Valencia D., Sasselov D. D., O'Connell R. J., 2007, ApJ, 656, 545
Wu Y., Goldreich P., 2002, ApJ, 564, 1024
Zhou J.-L., Lin D. N. C., 2008, in Sun Y.-S., Ferraz-Mello S., Zhou J-L., eds, Proc. IAU Symp. 249, Exoplanets: Detection, Formation and Dynamics. Cambridge Univ. Press, Cambridge, p. 285

This paper has been typeset from a TEX/LATEX file prepared by the author.